Transition quadrupole moments in superdeformed bands

B. Buck and A. C. Merchant
Department of Physics, University of Oxford, Theoretical Physics, 1 Keble Road, Oxford OX1 3NP, United Kingdom

S. M. Perez
Department of Physics, University of Cape Town, Private Bag, Rondebosch 7700, South Africa
(Received 13 April 2000; published 19 December 2000)

We have recently proposed a method to select core and cluster in a binary component description of atomic nuclei. The choice is based on the mismatch between measured binding energies and the underlying trend supplied by the liquid drop model. A key point is that the charge to mass ratios of parent, core, and cluster should be as nearly equal as possible. This approach implies that superdeformation should be ubiquitous across the Periodic Table. In these binary models, the transition quadrupole moments Q_t of superdeformed (SD) bands depend strongly on the charge and mass splits, but are rather insensitive to other details. In fact, given the cluster charge $\langle Z_2 \rangle$, Q_t can be determined algebraically. We compare calculations of transition quadrupole moments with the measured values for the 41 SD bands in 21 even-even nuclei for which experimental data are available. The mass range is from $A \sim 60$ to $A \sim 240$ and the values of Q_t vary from ~ 3 e b to ~ 30 e b. A good level of agreement is obtained.

DOI: 10.1103/PhysRevC.63.014312 PACS number(s): 21.60.Ev, 21.60.Gx, 23.20.Js, 27.90.+b

I. INTRODUCTION

After their initial observation in ^{152}Dy by Twin *et al.* [1], bands of superdeformed (SD) states were found in abundance in four distinct regions of the Periodic Table, near $A = 80$, 130, 150, and 190. In addition, Svensson *et al.* [2,3] have recently found SD bands in the $A \sim 60$ region. Since the fission isomers at $A \sim 230$ may also be regarded as examples of superdeformation, it is clear that the occurrence of this feature is truly widespread. We can thus say that many nuclei ranging in mass from $A \sim 60$ to $A \sim 240$ [4,5] have bands of states which exhibit superdeformation.

These observations are well explained by theoretical calculations employing the macroscopic-microscopic method of Strutinsky [6–8], which in many cases predated the experimental work. Satisfactory descriptions of superdeformation in the $A \sim 60$ region in terms of the configuration-dependent shell-correction approach with the cranked Nilsson potential [9] and the cranked relativistic mean field formalism [10] have also been given. In addition a generator coordinate method treatment of superdeformation has been proposed by Dancer *et al.* [11].

Nevertheless, many of the detailed properties of these bands remain obscure. Because the linking transitions to other, well-established states are rarely seen, it is usually the case that neither the excitation energies, nor even the spin values of the SD states are precisely determined. This makes a detailed comparison between experiment and theory difficult. Often the main evidence of superdeformation is a large transition quadrupole moment Q_t. It is the purpose of this paper to point out that a systematic reproduction of the measured values of Q_t for the 41 SD bands in 21 even-even nuclei listed in Ref. [5] can be obtained from a simple algebraic formula arising from a binary cluster model. This model is plainly phenomenological rather than microscopic, but transparently clear, intuitively appealing, and simple enough to be accessible to nonexperts. The use of the formula requires only the identification of the two components into which a given nucleus is to be decomposed and a radius parameter common to all the 41 cases considered.

II. CLUSTER SELECTION

We suggest [12,13] that likely binary clusterizations of a given parent nucleus can be identified from the local maxima of the function $D(Z_1,A_1,Z_2,A_2)$ defined by

$$D(Z_1,A_1,Z_2,A_2)=[B_E(Z_1,A_1)-B_L(Z_1,A_1)] + [B_E(Z_2,A_2)-B_L(Z_2,A_2)], \quad (1)$$

where B_E is an experimentally determined binding energy, and B_L the corresponding liquid drop value for each of the fragments of (charge, mass) (Z_i,A_i) with $i=1,2$ into which the parent of (charge, mass) (Z_T,A_T) may be divided. This means we are searching for the largest deviations of the summed binding energies of the two fragments from the underlying trend, as given by liquid drop values, in a two-dimensional (Z_1,A_1) landscape. A convenient form for B_L is [16]

$$B_L = a_v A - a_s A^{2/3} - a_c \frac{Z^2}{A^{1/3}} - a_a \frac{(A-2Z)^2}{A} + \delta, \quad (2)$$

where

$$a_v = 15.56 \text{ MeV}, \quad a_s = 17.23 \text{ MeV}, \quad a_c = 0.697 \text{ MeV}, \quad a_a = 23.285 \text{ MeV}. \quad (3)$$

The pairing term δ in Eq. (2) is taken as $12/\sqrt{A}$ MeV because in this paper we consider only the fragmentation of even-even nuclei into even-even fragments.

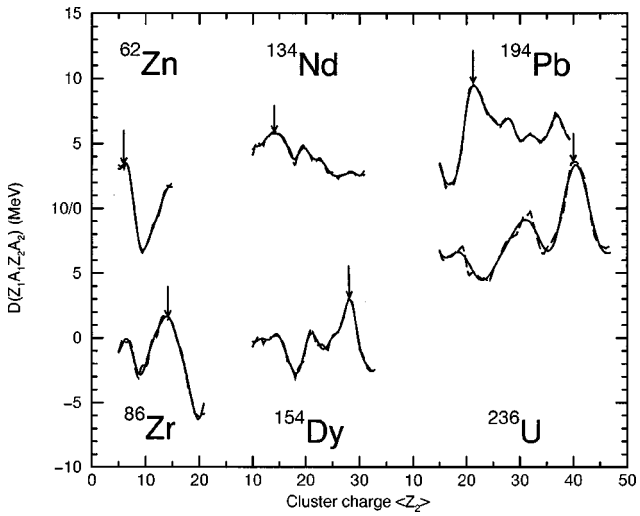

FIG. 1. Calculations of $\langle D(Z_1,A_2,Z_2,A_2)\rangle$ as a function of cluster charge $\langle Z_2\rangle$ for ^{62}Zn, ^{86}Zr, ^{134}Nd, ^{154}Dy, ^{194}Pb, and ^{236}U. Dashed curve: full calculation; full curve: smoothed calculation. Arrows indicate the preferred cluster charge.

We can reduce our search to one dimension by restricting attention to fragments which have the same charge to mass ratio as the parent nucleus, so that they obey the condition

$$\frac{Z_1}{A_1}=\frac{Z_2}{A_2}=\frac{Z_T}{A_T} \tag{4}$$

as closely as possible. This restriction is motivated by the experimental observation that electric dipole transitions in even-even nuclei are found to be very weak. This comes about in our cluster model because the proposed constraint forces the centers of mass and charge to be coincident. The appropriate operator for dipole transition rates involves the multiplicative factor $(Z_1/A_1-Z_2/A_2)$, so that even though the mass asymmetry between the two clusters may be very large $(A_1 \gg A_2)$, the electric dipole transition rates still vanish identically. That the centers of charge and mass in the nucleus almost coincide is an effect of the strong neutron-proton force. In general, no single choice of cluster can satisfy this dipole constraint exactly. However, if we are willing to consider that the nuclear state is a superposition of several possible cluster partitions then it becomes feasible to satisfy Eq. (4) by using effective or average cluster charges and masses [13]. To keep things as simple as possible, we use the even-even cluster closest to this average in what follows.

Figure 1 shows $D(Z_1,A_1,Z_2,A_2)$ as a function of cluster charge $\langle Z_2\rangle$ for six nuclei representative of the mass regions where SD bands have been reported. The behavior illustrated is completely typical of most of the nuclei we have examined to date, which leads us to expect bands of strongly deformed states essentially everywhere. In our model the deformation of the parent nucleus is related to the ratio r of cluster to total mass (or charge). Values of $r \lesssim 1/6$ are associated with normally deformed ground state bands [13–15,17,18], and larger values indicate larger deformations. In Fig. 1 we thus apply cutoffs at $\langle Z_2\rangle = 5$, 10, and 15 for nuclei in the charge ranges 30–40, 58–66, and 80–92, respectively, and take the most prominent local maximum of the resulting D plot to indicate the most likely SD cluster in the parent nucleus (at an excitation energy which we are, at present, unable to determine). Collective motion of this structure gives rise to SD bands in the parent nucleus.

Experiment often shows several SD bands in a given nucleus, sometimes with similar values of Q_t, but also with different ones. In microscopic terms this is explained in terms of particle-hole structures, and the blocking of single-particle level crossings in highly rotating nuclei. It can be interpreted in our model as follows. We expect several bands with very similar quadrupole deformations associated with any given cluster structure because excitations of cluster or core or both can all produce closely related bands with comparable excitation energies. The significance of the lesser maxima of $D(Z_1,A_1,Z_2,A_2)$ is currently under investigation, but we strongly suspect that bands associated with these clusterizations may be present as well. This would lead to the coexistence of several clusterizations in the same nucleus marked out by their different quadrupole deformations. At the moment we cannot tie a given observed band uniquely to a given clusterization, but the measurement of linking transitions to known bands would enable this to be done.

The SD clusterizations presented in Table I result from a straightforward and rigorous application of the above criteria. Very often this yields a completely unambiguous result for the preferred superdeformed clusterization. However, there are a few cases where the choice is not clear cut, and additional criteria such as Q values and cluster penetrability of the Coulomb barrier need to be considered. For example, in each of the lightest nuclei, ^{60,62}Zn and ^{80,82}Sr, the preferred D maximum at $\langle Z_2\rangle = 6$ is very close to the cutoff, and in Table II we show the effect of choosing another prominent D maximum of almost equal magnitude in the region of interest which occurs at $\langle Z_2\rangle = 14$. We note that although $\langle Z_2\rangle = 6$ gives a better fit to the transition quadrupole moments Q_t in the present work, a more microscopic calculation for ^{60}Zn (which includes fitting the SD spectrum) suggests that $\langle Z_2\rangle = 14$ may be better overall [15].

We also note that no maxima stand out strongly for ^{132}Ce or ^{134}Nd, our two nuclei in the $A \approx 130$ region. The most prominent of these maxima in each case is at $\langle Z_2\rangle = 14$, and results in far too large a value for Q_t. For these nuclei we supplement our considerations by calculating half-lives for cluster emission (as done in a previous study of some heavier isotopes of Ce and Nd [18], where details may be found). Taking the shortest half-lives to indicate the most likely clusters we propose an ^{16}O cluster structure for both these nuclei, leading to the results of Table II. The question of how best to choose a cluster for an arbitrary parent nucleus is not yet completely answered, and is an ongoing problem. In addition to ourselves, several other groups have worked on this problem [19–21].

III. TRANSITION QUADRUPOLE MOMENTS

There is a well-known relationship between the charge radii of a given nucleus and the core and cluster into which it is decomposed (see, for example, Ref. [22]) of the form

TABLE I. Transition quadrupole moments (expected clusterizations).

Nucleus	Q_t(calc) (e b)	Q_t(expt) [4,5] for different observed bands. (e b)
^{60}Zn=^{48}Cr+^{12}C	2.5±0.1	2.75±0.45
^{62}Zn=^{50}Cr+^{12}C	2.6±0.1	$2.7^{+0.7}_{-0.5}$
^{80}Sr=^{68}Ge+^{12}C	3.2±0.1	$2.7^{+0.7}_{-0.6}$; $2.2^{+0.6}_{-0.5}$; $2.8^{+1.1}_{-0.8}$; $3.6^{+2.0}_{-1.1}$
^{82}Sr=^{70}Ge+^{12}C	3.3±0.2	4.5±0.9
^{84}Zr=^{56}Fe+^{28}Si	5.9±0.2	5.2±0.8
^{86}Zr=^{58}Fe+^{28}Si	6.0±0.2	$4.6^{+0.7}_{-0.6}$; 4.0±0.3; $3.8^{+0.6}_{-0.5}$; $5.4^{+2.2}_{-1.1}$
^{132}Ce=^{100}Ru+^{32}Si	9.5±0.3	7.4±0.4; 7.3±0.3; 7.6±0.4
^{134}Nd=^{102}Pd+^{32}Si	9.8±0.3	6.8±0.3; 6.4±0.4
^{142}Sm=^{88}Sr+^{54}Cr	13.6±0.5	11.7±0.1; $13.2^{+0.8}_{-0.7}$
^{146}Gd=^{90}Zr+^{56}Cr	14.2±0.5	12±2
^{148}Gd=^{88}Sr+^{60}Fe	14.7±0.5	14.6±0.2; 14.8±0.3; 17.8±1.3
^{150}Gd=^{88}Sr+^{62}Fe	14.8±0.5	$17.0^{+0.5}_{-0.4}$; $17.4^{+0.5}_{-0.4}$; 16.2±0.4; $15.0^{+0.6}_{-0.4}$; 16.8±1.2
^{152}Dy=^{88}Sr+^{64}Ni	15.6±0.6	17.5±0.5
^{154}Dy=^{88}Sr+^{66}Ni	15.7±0.6	$15.9^{+3.1}_{-2.1}$
^{190}Hg=^{142}Nd+^{48}Ca	17.1±0.6	$17.7^{+1.0}_{-1.2}$; 17.6±1.5
^{192}Hg=^{140}Ce+^{52}Ti	18.1±0.6	20.2±1.2; 19.5±1.5
^{194}Hg=^{140}Ce+^{54}Ti	18.4±0.7	17.7±0.4; 17.6±0.6; 17.6±0.8
^{194}Pb=^{144}Nd+^{50}Ti	18.3±0.7	$20.1^{+0.3}_{-0.5}$
^{196}Pb=^{144}Nd+^{52}Ti	18.6±0.7	$19.5^{+0.4}_{-0.3}$
^{236}U=^{134}Te+^{102}Zr	29.3±1.1	32±5
^{238}U=^{134}Te+^{104}Zr	29.5±1.1	29±3

$$(Z_1+Z_2)\langle R^2\rangle = Z_1\langle R_1^2\rangle + Z_2\langle R_2^2\rangle + \alpha_2\langle r_{L,L}^2\rangle, \tag{5}$$

where (Z_i, A_i) are as defined in the previous section, $\langle R^2\rangle$, $\langle R_1^2\rangle$, and $\langle R_2^2\rangle$ are mean square charge radii for the parent, core, and cluster nuclei, respectively,

$$\alpha_2 = \frac{Z_1A_2^2 + Z_2A_1^2}{(A_1+A_2)^2}, \tag{6}$$

and

$$\langle r_{L,L}^2\rangle = \int_0^\infty r^2|\chi_L(r)|^2\, dr \tag{7}$$

with $\chi_L(r)$ the radial wave function for the relative motion of cluster and core with angular momentum L ($L=0$ for positive parity bandheads in even-even nuclei). For internally unexcited even-even cluster and core, the total angular momentum is identical to the relative orbital angular momentum of the two bodies and so the transition quadrupole moment for states $J=L+2$ and $J=L$ is simply

$$Q_t = 2\alpha_2\langle r_{L+2,L}^2\rangle, \tag{8}$$

where

$$\langle r_{L+2,L}^2\rangle = \int_0^\infty r^2\chi_L^*(r)\chi_{L+2}(r)dr. \tag{9}$$

Cluster bands are characterized by a large value of the quantum number $G=2n+L$, so that the radial wave functions for states with low angular momentum L have a large number of nodes n. Clearly, the radial functions for states with $J=L+2$ and $J=L$ differ in their node number by one. However,

TABLE II. Transition quadrupole moments (alternative clusterizations).

Nucleus	Q_t(calc) (e b)	Q_t(expt) [4,5] for different observed bands (e b)
^{60}Zn=^{32}S+^{28}Si	3.9±0.2	2.75±0.45
^{62}Zn=^{34}S+^{28}Si	4.0±0.2	$2.7^{+0.7}_{-0.5}$
^{80}Sr=^{52}Cr+^{28}Si	5.5±0.2	$2.7^{+0.7}_{-0.6}$; $2.2^{+0.6}_{-0.5}$; $2.8^{+1.1}_{-0.8}$; $3.6^{+2.0}_{-1.1}$
^{82}Sr=^{54}Cr+^{28}Si	5.6±0.2	4.5±0.9
^{132}Ce=^{116}Sn+^{16}O	6.0±0.2	7.4±0.4; 7.3±0.3; 7.6±0.4
^{134}Nd=^{118}Xe+^{16}O	6.2±0.2	6.8±0.3; 6.4±0.4

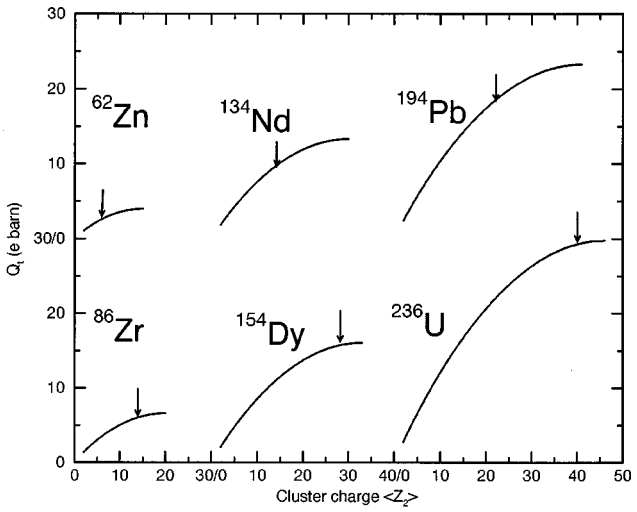

FIG. 2. Calculations of transition quadrupole moment Q_t (e b) as a function of cluster charge $\langle Z_2 \rangle$ for ^{62}Zn, ^{86}Zr, ^{134}Nd, ^{154}Dy, ^{194}Pb, and ^{236}U. Arrows indicate the cluster charge suggested by the D plots of Fig. 1.

we have previously shown that [23], even up to rather high L values, such pairs of radial functions are practically identical, except very close to the origin ($r=0$) where the extra node is accommodated. It is therefore a good approximation to replace $\langle r^2_{L+2,L} \rangle$ by $\langle r^2_{L,L} \rangle$ and write

$$Q_t \approx 2[(Z_1+Z_2)\langle R^2 \rangle - Z_1 \langle R_1^2 \rangle - Z_2 \langle R_2^2 \rangle]. \qquad (10)$$

If, in addition, the mean square charge radius of each of the nuclei may be related to its mass by $\langle R_i^2 \rangle = R_0^2 A_i^{2/3}$ then this simplifies to

$$Q_t \approx 2R_0^2[Z_T A_T^{2/3} - Z_1 A_1^{2/3} - Z_2 A_2^{2/3}] \qquad (11)$$

which enables us to evaluate Q_t once the core-cluster binary decomposition of the parent nucleus has been chosen and a value for R_0 specified.

We take $R_0 = 1.07 \pm 0.02$ fm, determined from elastic electron scattering by Ravenhall [24] as the radius parameter of a Fermi density distribution for heavy nuclei. The resulting values for Q_t are compared with experiment in Tables I and II. We note the large number of magic proton and neutron values amongst the cores and clusters in Tables I and II (reflecting the associated increase in stability). Thus there are magic proton numbers in the isotopes of O, Ca, Ni, and Sn of 8, 20, 28, and 50, respectively. Also there are magic neutron numbers in ^{16}O, ^{48}Ca, ^{88}Sr, ^{90}Zr, ^{134}Te, ^{140}Ce, and ^{142}Nd of 8, 28, 50, 50, 82, 82, and 82, respectively.

Figure 2 shows the variation of Q_t with cluster charge, according to Eq. (11), for the same six nuclei examined in Fig. 1. We have taken $R_0 = 1.07$ fm and related A_i to Z_i by means of Eq. (4). It is apparent that Q_t is rather sensitive to the core-cluster decomposition, ranging from about 1 to 4 e b in ^{62}Zn as the cluster goes from He to Si, and from about 2 to 29 e b in ^{236}U as the cluster goes from He to Zr. This makes it all the more astonishing that a formula as simple as Eq. (11) can account for the measured Q_t values in so many nuclei.

Equation (11) for Q_t takes no account of the angular momentum of the SD states. However, previous experience suggests that Q_t will decrease somewhat with increasing J. Our work in actinide nuclei [25] shows a small but systematic decrease of $\langle r^2_{L+2,L} \rangle$, the quantity which ought to be used to evaluate Q_t, in all nuclei which were examined. This centrifugal antistretching may explain why rather large error bars have been attributed to Q_t values deduced from long sequences of SD states. They reflect a genuine change in value of Q_t between the band members with the highest and lowest known spins. In addition to these statistical errors, Beausang *et al.* [26] warn that stopping power uncertainties of 10–20 % are also to be expected.

To calculate other properties of SD states, more detailed calculations are necessary. In principle this is a relatively straightforward task. Once core and cluster have been identified, we can solve a Schrödinger equation for their relative motion using a universal form for the ion-ion potential [27]. A value for the relative motion quantum number $G = 2n + L$ can also be assigned from systematic considerations [14]. Then energies and wave functions are available for the calculation of whichever observables are desired. However, the details of such calculations depend on the precise excitation energy of the bandhead and the value of G employed. To attain maximum accuracy in these matters it is best to fine tune the potential radius and G value so as to reproduce the experimental excitation energies of a couple of states of known angular momentum. Because linking transitions between SD and ND bands are rarely seen, this information is not often available (although we have performed such calculations for ^{60}Zn [15], ^{194}Hg, ^{236}U, and ^{240}Pu [14], some of the rare examples where it is possible). We hope that this situation will gradually improve as more experimental data are gathered.

IV. CONCLUSIONS

We have applied a principle of maximum stability to determine the most favored core-cluster decompositions of the 21 even-even nuclei for which transition quadrupole moments Q_t of superdeformed bands have been measured. In two cases where this is inconclusive (namely ^{132}Ce and ^{134}Nd) we have supplemented it by consideration of the calculated half-life for cluster emission. Once the clusterization has been specified, we have used a simple algebraic formula to calculate Q_t, viz. Eq. (11). The single adjustable parameter R_0 was taken as 1.07 ± 0.2 fm from Ravenhall's fits to elastic electron scattering from heavy nuclei [24]. A generally good account was given of the data.

ACKNOWLEDGMENTS

A.C.M. would like to thank the U.K. Engineering and Physical Science Research Council (EPSRC) for financial support. S.M.P. would like to thank the S.A. Foundation for Research, and the University of Cape Town for financial support.

[1] P. J. Twin *et al.*, Phys. Rev. Lett. **57**, 811 (1986).
[2] C. E. Svensson *et al.*, Phys. Rev. Lett. **79**, 1233 (1997).
[3] C. E. Svensson *et al.*, Phys. Rev. Lett. **82**, 3400 (1999).
[4] B. Singh, R. B. Firestone, and S. Y. Frank Chu, Nucl. Data Sheets **78**, 1 (1996).
[5] Xiao-Ling Han and Cheng-Li Wu, At. Data Nucl. Data Tables **73**, 43 (1999).
[6] J. Dudek, W. Nazarewicz, Z. Szymanski, and G. A. Leander, Phys. Rev. Lett. **59**, 1405 (1987)
[7] W. Satuła, J. Dobaczewski, J. Dudek, and W. Nazarewicz, Phys. Rev. Lett. **77**, 5182 (1996).
[8] T. R. Werner and J. Dudek, At. Data Nucl. Data Tables **50**, 179 (1992); **59**, 1 (1995).
[9] T. Bengtsson and I. Ragnarsson, Nucl. Phys. **A436**, 14 (1985).
[10] A. V. Afanasjev, J. König, and P. Ring, Nucl. Phys. **A608**, 107 (1996).
[11] H. Dancer, S. Perriés, P. Bonche, H. Flocard, P.-H. Heenen, J. Meyer, and M. Meyer, Nucl. Phys. **A654**, 655c (1999).
[12] B. Buck, A. C. Merchant, and S. M. Perez, Few-Body Syst. **29**, 53 (2000).
[13] B. Buck, A. C. Merchant, M. J. Horner, and S. M. Perez, Phys. Rev. C **61**, 024314 (2000).
[14] B. Buck, A. C. Merchant, M. J. Horner, and S. M. Perez, Nucl. Phys. **A673**, 157 (2000).
[15] B. Buck, A. C. Merchant, and S. M. Perez, Phys. Rev. C **61**, 014310 (2000).
[16] W. S. C. Williams, in *Nuclear and Particle Physics* (Clarendon, Oxford, 1991), p. 60.
[17] B. Buck, A. C. Merchant, and S. M. Perez, Nucl. Phys. **A652**, 211 (1999).
[18] B. Buck, A. C. Merchant, and S. M. Perez, Nucl. Phys. **A657**, 267 (1999).
[19] J. Cseh and W. Scheid, J. Phys. G **18**, 1419 (1992).
[20] J. Zhang, W. D. M. Rae, and A. C. Merchant, Nucl. Phys. **A575**, 61 (1994).
[21] T. M. Shneidman, G. G. Adamian, N. V. Antonenko, S. P. Ivanova, and W. Scheid, Nucl. Phys. **A671**, 119 (2000).
[22] B. Buck and A. A. Pilt, Nucl. Phys. **A280**, 133 (1977).
[23] B. Buck, A. C. Merchant, and S. M. Perez, Phys. Rev. C **57**, R2095 (1998).
[24] D. G. Ravenhall, Rev. Mod. Phys. **30**, 430 (1958)
[25] B. Buck, A. C. Merchant, and S. M. Perez, Phys. Rev. C **59**, 750 (1999); J. Phys. G **25**, 901 (1999).
[26] C. W. Beausang *et al.*, Phys. Lett. B **417**, 13 (1998).
[27] B. Buck, A. C. Merchant, and S. M. Perez, Nucl. Phys. **A614**, 129 (1997).